— Supplementary information—
An Interaction-Driven Many-Particle Quantum Heat Engine And Its Universal Behavior

Yang-Yang Chen,[1,2] Gentaro Watanabe,[3] Yi-Cong Yu,[2] Xi-Wen Guan,[2,4,*] and Adolfo del Campo[5,6,7,8,†]

[1] *Shenzhen Institute for Quantum Science and Engineering, and Department of Physics, Southern University of Science and Technology, Shenzhen 518055, China*
[2] *State Key Laboratory of Magnetic Resonance and Atomic and Molecular Physics, Wuhan Institute of Physics and Mathematics, Chinese Academy of Sciences, Wuhan 430071, China*
[3] *Department of Physics and Zhejiang Institute of Modern Physics, Zhejiang University, Hangzhou, Zhejiang 310027, China*
[4] *Department of Theoretical Physics, Research School of Physics and Engineering, Australian National University, Canberra ACT 0200, Australia*
[5] *Donostia International Physics Center, E-20018 San Sebastián, Spain*
[6] *IKERBASQUE, Basque Foundation for Science, E-48013 Bilbao, Spain*
[7] *Department of Physics, University of Massachusetts, Boston, MA 02125, USA*
[8] *Theoretical Division, Los Alamos National Laboratory, Los Alamos, NM 87545, USA*

Contents

I. 1D BOSE GASES IN A HARD WALL POTENTIAL

Consider a system with N identical bosons with a contact interaction confined in a one-dimensional (1D) hard-wall potential. This system is described by the Hamiltonian

$$H = -\frac{\hbar^2}{2m}\sum_{i=1}^{N}\frac{\partial^2}{\partial x_i^2} + g_{1\mathrm{D}}\sum_{1\le i<j\le N}\delta(x_i - x_j)\,, \tag{1}$$

where $g_{1\mathrm{D}} = \hbar^2 c/m$ is the 1D coupling constant and c parametrizes the interaction strength. Hereafter, we set $\hbar = 2m = 1$. This model can be exactly solved by the Bethe ansatz [1, 2], and the wavefunction is given by

$$\Psi_{\{\epsilon_i k_i\}}(x_1, \cdots, x_N) = \sum_{\epsilon_1,\cdots,\epsilon_N}\sum_{P}\epsilon_1\cdots\epsilon_N\, A(\epsilon_1 k_{P_1}, \cdots, \epsilon_N k_{P_N})\, e^{i(\epsilon_1 k_{P_1} x_1 + \cdots + \epsilon_N k_{P_N} x_N)}\,, \tag{2}$$

*Electronic address: xwe105@wipm.ac.cn
†Electronic address: adolfo.delcampo@umb.edu

where the sum is taken over all $N!$ permutations P of N integers such that $P:(1,2,\cdots,N)\to(P_1,P_2,\cdots P_N)$, and ϵ_i takes ±1. Here, k_{P_i} is the the wave number which satisfies the Bethe equations

$$e^{i2k_iL}=-\prod_{j=1}^{N}\frac{(k_i-k_j+ic)(k_i+k_j+ic)}{(k_i-k_j-ic)(k_i+k_j-ic)}\qquad(i=1,\cdots,N)\,, \tag{3}$$

and the energy of this state is given by

$$E=\sum_{i=1}^{N}k_i^2\,. \tag{4}$$

Taking the logarithm of the Bethe equations (3), one obtains

$$Lk_i=\pi I_i-\sum_{j\neq i}\left(\arctan\frac{k_i-k_j}{c}+\arctan\frac{k_i+k_j}{c}\right)\qquad(i=1,\cdots,N)\,, \tag{5}$$

where $\{I_i\}$ are integer quantum numbers, which are arranged in ascending order: $1\le I_1\le\cdots\le I_N$. Thus, the wave numbers $\{k_i\}$ are also in ascending order, i.e., $0<k_1<\cdots<k_N$.

Scaling invariant behavior

We next focus on the low energy excitations which dominate the thermodynamics in the strongly-interacting Bose gas at low temperature. A Taylor expansion of the rhs of Eq. (5) for $c\gg k_N$ yields the following asymptotic solution

$$\begin{aligned}
Lk_i &= \pi I_i-\sum_{i\neq j}^{N}\left[\frac{k_i-k_j}{c}+\frac{k_i+k_j}{c}\right]+O\left(\frac{k_N^3}{c^3}\right)\\
&= \pi I_i+\frac{2(1-N)k_i}{c}+O\left(\frac{k_N^3}{c^3}\right)\\
&\approx \pi I_i+\frac{2(1-N)}{c}\left[\frac{\pi I_i}{L}+\frac{2(1-N)\pi I_i}{cL^2}\right]+O\left(\frac{k_N^3}{c^3}\right)\\
&\approx \pi\left[1+\frac{2(1-N)}{cL}+\frac{4(1-N)^2}{c^2L^2}\right]I_i+O\left(\frac{k_N^3}{c^3}\right).
\end{aligned} \tag{6}$$

Note that, in this regime, the dependence of the quasimomentum k_i on the other quasimomenta k_j with $j\neq i$ is of higher order in k_N/c. In this sense, the algebraic Bethe ansatz equations (5) decouple in this limit.

The energy eigenvalue $\varepsilon_n(c)$ for a given set of quantum numbers $\mathcal{I}_n\equiv\{I_i^{(n)}\}$ is set by

$$\begin{aligned}
\varepsilon_n(c) &\approx \sum_{i=1}^{N}k_i^2\\
&\approx \frac{\pi^2}{L^2}\left[1-\frac{4(N-1)}{cL}+\frac{12(N-1)^2}{c^2L^2}\right]\sum_{i=1}^{N}{I_i^{(n)}}^2+\frac{1}{L^2}O\left(\frac{k_N^3}{c^3}\right).
\end{aligned} \tag{7}$$

Thus, up to corrections of order $1/c^2$, the energy eigenvalue can be written in terms of that of free fermions rescaled by an overall factor resulting from the interactions. We refer to this factor as the generalized exclusion statistics parameter, in view of [3], and define it as

$$\lambda_c=1-\frac{4(N-1)}{cL}+\frac{12(N-1)^2}{c^2L^2}\,. \tag{8}$$

Using it, the energy eigenvalues of a strongly-interacting 1D Bose gases simply read

$$\varepsilon_n(c)\approx\frac{\pi^2\lambda_c}{L^2}\sum_{i=1}^{N}{I_i^{(n)}}^2\,, \tag{9}$$

and exhibit the scale-invariant behavior

$$\frac{\varepsilon_n(c)}{\varepsilon_n(c')}=\frac{\lambda_c}{\lambda_{c'}}\,. \tag{10}$$

II. ENERGIES OF EQUILIBRIUM AND NON-EQUILIBRIUM STATES

The equilibrium state of the system at temperature T can be characterized by the partition function

$$Z = \sum_{n=1}^{\infty} e^{-\varepsilon_n(c)/T}\,, \tag{11}$$

where the summation is taken over all the quantum states. The average energy of the system is given by

$$\varepsilon_{\rm eq}(c,T) = \sum_{n=1}^{\infty} p_n(c,T)\,\varepsilon_n(c)\,, \tag{12}$$

with $p_n(c,T)$ being the probability measure of the n-th eigenstate in the Gibbs ensemble given by

$$p_n(c,T) = e^{-\varepsilon_n(c)/T}/Z\,. \tag{13}$$

During the interaction-driven strokes, the system generally deviates from the initial equilibrium state as a result of the modulation of the interaction strength c. However, since the energy gap for low-energy excitations is nonzero in the system with finite N bosons, a sufficiently slow ramping process becomes adiabatic and keeps the probability distribution $p_n(c,T)$ unchanged. Therefore, for the non-equilibrium state resulting from an adiabatic ramping process, the average energy of the system at the interaction parameter c' is given by

$$\varepsilon_{\rm neq}(c';c,T) = \sum_{n=1}^{\infty} p_n(c,T)\,\varepsilon_n(c')\,. \tag{14}$$

Due to the scale-invariant behavior at strong coupling, the energy of the non-equilibrium state at the end of the interaction-ramp isentropic process is found to be

$$\varepsilon_{\rm neq}(c';c,T) = \frac{\lambda_{c'}}{\lambda_c}\,\varepsilon_{\rm eq}(c,T)\,. \tag{15}$$

Furthermore, the scale-invariant behavior Eq. (10) indicates that we can relate a non-equilibrium state in adiabatic interaction-driven processes to an equilibrium state with an effective temperature T' by noting that

$$\begin{aligned}
\varepsilon_{\rm neq}(c';c,T) &= \sum_{n=1}^{\infty} \frac{e^{-\varepsilon_n(c)/T}}{\sum_{m=1}^{\infty} e^{-\varepsilon_m(c)/T}}\,\varepsilon_n(c') \\
&= \sum_{n=1}^{\infty} \frac{e^{-\varepsilon_n(c')\lambda_c/T\lambda_{c'}}}{\sum_{m=1}^{\infty} e^{-\varepsilon_m(c')\lambda_c/T\lambda_{c'}}}\,\varepsilon_n(c') \\
&= \varepsilon_{\rm eq}(c',T')\,,
\end{aligned} \tag{16}$$

where the effective temperature reads

$$T' = \lambda_{c'}T/\lambda_c\,. \tag{17}$$

III. QUANTUM HEAT ENGINE

For the interaction-driven quantum heat engine (see Fig. 1 in the main text), the heat absorbed from the hot reservoir is given by

$$\begin{aligned}
Q_2 &= \varepsilon_{\rm eq}(c_{\rm B},T_{\rm C}) - \varepsilon_{\rm neq}(c_{\rm B};c_{\rm A},T_{\rm A}) \\
&= \varepsilon_{\rm eq}(c_{\rm B},T_{\rm C}) - \frac{\lambda_{c_{\rm B}}}{\lambda_{c_{\rm A}}}\,\varepsilon_{\rm eq}(c_{\rm A},T_{\rm A})\,,
\end{aligned} \tag{18}$$

while the heat released from the engine to the cold reservoir reads

$$\begin{aligned} Q_4 &= \varepsilon_{\rm neq}(c_{\rm A}; c_{\rm B}, T_{\rm C}) - \varepsilon_{\rm eq}(c_{\rm A}, T_{\rm A}) \\ &= \frac{\lambda_{c_{\rm A}}}{\lambda_{c_{\rm B}}}\, \varepsilon_{\rm eq}(c_{\rm B}, T_{\rm C}) - \varepsilon_{\rm eq}(c_{\rm A}, T_{\rm A})\,. \end{aligned} \tag{19}$$

Therefore, the efficiency η and the work W done by the engine are given by

$$\eta = 1 - \frac{Q_4}{Q_2} = 1 - \frac{\lambda_{c_{\rm A}}}{\lambda_{c_{\rm B}}}\,, \tag{20}$$

$$W = Q_2 - Q_4 = \left(1 - \frac{\lambda_{c_{\rm A}}}{\lambda_{c_{\rm B}}}\right) Q_1\,. \tag{21}$$

The efficiency η and work W can also be obtained numerically by solving Eq. (5). In our calculations, we take a proper cutoff for excited states whose probability p_n given by Eq. (13) is much smaller than that of the ground state. The efficiency of the interaction-driven cycle is set by the energy ratio between the isolated strokes. This feature is as well shared by the harmonic Otto cycle. Here we would like to remark that the conventional definition of an Otto cycle involves expansion and compression strokes by definition. A generalized notion of Otto cycle has been considered in the literature, e.g. see section 25.2.2 of the reference [4]. Whenever the Hamiltonian is proportional to a scaling function $g(\gamma)$, $\hat{H} = g(\gamma)\hat{h}$, the efficiency of an Otto like cycle based on a change of the parameter γ reads $\eta = 1 - \frac{\min g(\gamma)}{\max g(\gamma)}$.

However, scale invariance cannot be taken for granted in an interaction-driven system. It is our contribution to establish that this is the case in an interacting Bose gas and effectively one-dimensional quantum liquids, i.e. Luttinger liquids acting as a working substance. The many-particle interaction-driven cycle proposed in this manuscript can be described an a generalized Otto cycle if an only if the spectrum is scale invariant. In this case, the role of c plays the role of the parameter γ and λ_c the role of $g(\gamma)$.

IV. THERMODYNAMIC LIMIT

In the laboratory, a Bose gas confined in an effectively 1D trap typically consists of thousands of particles. It is generally considered that such system is well described by the thermodynamic limit, i.e., N and $L \to \infty$ with $n = N/L$ being kept constant. The equilibrium states can then be described by the Yang-Yang thermodynamic equation [5]. The pressure p, particle density n, entropy density s and internal energy density $\mathcal{E}$ can then be found as described in the text.

Note that we take the thermodynamic limit after the slow ramping limit to guarantee that no diabatic transitions occur during the ramping processes. Thus, the probability $p_n(c, T)$ is unchanged during the ramping processes. In these processes, the entropy should also be constant because no heat is transferred in or out of the working substance. Given the expressions for the heat absorbed during the hot isochore stroke (B to C)

$$Q_2 = L\left[\mathcal{E}(c_{\rm B}, T_{\rm C}) - \mathcal{E}(c_{\rm B}, T_{\rm B})\right] \tag{22}$$

and the heat released during the cold isochore stroke (D to A)

$$Q_4 = L\left[\mathcal{E}(c_{\rm A}, T_{\rm D}) - \mathcal{E}(c_{\rm A}, T_{\rm A})\right]\,, \tag{23}$$

the efficiency η and work output W are given by

$$\eta = 1 - \frac{\mathcal{E}(c_{\rm A}, T_{\rm D}) - \mathcal{E}(c_{\rm A}, T_{\rm A})}{\mathcal{E}(c_{\rm B}, T_{\rm C}) - \mathcal{E}(c_{\rm B}, T_{\rm B})}\,, \tag{24}$$

$$W = L\left[\mathcal{E}(c_{\rm B}, T_{\rm C}) - \mathcal{E}(c_{\rm B}, T_{\rm B}) - \mathcal{E}(c_{\rm A}, T_{\rm D}) + \mathcal{E}(c_{\rm A}, T_{\rm A})\right]\,. \tag{25}$$

Here, $T_{\rm B}$ and $T_{\rm D}$ can be determined using the fact that the interaction-driven strokes are isentropic, namely

$$s(c_{\rm A}, T_{\rm A}) = s(c_{\rm B}, T_{\rm B}), \quad s(c_{\rm B}, T_{\rm C}) = s(c_{\rm A}, T_{\rm D})\,, \tag{26}$$

where $T_{\rm A}$ and $T_{\rm C}$ denote the temperature of the cold and hot reservoir, respectively. The efficiency can thus be obtained numerically by solving the TBA equation, see Methods.

Universality at low energies

The low-energy physics of 1D Bose gases can be well captured by the Luttinger liquid theory. The free energy density $\mathcal{F}$ is given by [6]

$$\mathcal{F} \approx \mathcal{E}_0 - \frac{\pi T^2}{6v_{\rm s}}\,, \tag{27}$$

where $\mathcal{E}_0$ is the energy density of the ground state, $v_{\rm s}$ is the sound velocity which depends on the particle density n and the interaction strength c. The entropy density s is given by the derivative of the free energy, namely,

$$s = -\frac{\partial \mathcal{F}}{\partial T} = \frac{\pi T}{3v_{\rm s}}\,. \tag{28}$$

The energy $\mathcal{E} = F + T\,s = \mathcal{E}_0 + \frac{\pi T^2}{6v_{\rm s}}$. The heat absorbed from the hot resevoir in the hot isochore stroke (B to C) is given by

$$Q_2 = L(\mathcal{E}_{\rm C} - \mathcal{E}_{\rm B}) = \frac{\pi L}{6v_{\rm s}^{\rm B}}(T_{\rm C}^2 - T_{\rm B}^2)\,, \tag{29}$$

and the heat released to the cold reservoir in the cold isochore stroke (D to A) is

$$Q_4 = L(\mathcal{E}_{\rm D} - \mathcal{E}_{\rm A}) = \frac{\pi L}{6v_{\rm s}^{\rm A}}(T_{\rm D}^2 - T_{\rm A}^2)\,. \tag{30}$$

By Eq. (26), we obtain

$$\frac{\pi T_{\rm A}}{3v_{\rm s}^{\rm A}} = \frac{\pi T_{\rm B}}{3v_{\rm s}^{\rm B}}\,, \quad \frac{\pi T_{\rm D}}{3v_{\rm s}^{\rm A}} = \frac{\pi T_{\rm C}}{3v_{\rm s}^{\rm B}}\,, \tag{31}$$

namely,

$$\frac{T_{\rm A}}{T_{\rm B}} = \frac{T_{\rm D}}{T_{\rm C}} = \frac{v_{\rm s}^{\rm A}}{v_{\rm s}^{\rm B}}\,. \tag{32}$$

To simplify, we introduce the following two dimensionless parameters:

$$\xi = \frac{v_{\rm s}^{\rm A}}{v_{\rm s}^{\rm B}}\,, \quad \kappa = \frac{T_{\rm A}}{T_{\rm C}}\,. \tag{33}$$

Since $T_{\rm A} < T_{\rm B} < T_{\rm C}$, we get

$$0 < \kappa < \xi < 1 \tag{34}$$

The work can be extracted from the heat engine is given by

$$\begin{aligned} W &= Q_2 - Q_4 \\ &= \frac{\pi L}{6v_{\rm s}^{\rm B}}(T_{\rm C}^2 - T_{\rm B}^2) - \frac{\pi L}{6v_{\rm s}^{\rm A}}(T_{\rm D}^2 - T_{\rm A}^2) \\ &= \frac{\pi L T_{\rm C}^2}{6v_{\rm s}^{\rm B}}(1-\xi)\left(1 - \frac{\kappa^2}{\xi^2}\right)\,. \end{aligned} \tag{35}$$

An interesting question is what is the optimal work extracted from this heat engine when the temperatures of the two reservoirs, $T_{\rm A}$ and $T_{\rm C}$, are fixed. It is easy to show that the work output W always has a maximum value (see the right panel of Fig. 1) at $\xi = \xi_{\rm c}$ with

$$\xi_{\rm c} = \frac{\kappa^2}{a^{1/3}} - \frac{a^{1/3}}{3}\,, \tag{36}$$

where $a = 27\kappa^2\left[\sqrt{1 + (\kappa^2/27)} - 1\right] \approx \kappa^4/2$. Thus for small $\kappa \ll 1$, we get

$$\xi_{\rm c} \approx (2\kappa^2)^{\frac{1}{3}}\left[1 - \frac{1}{3}\left(\frac{\kappa}{2}\right)^{\frac{2}{3}}\right]\,. \tag{37}$$

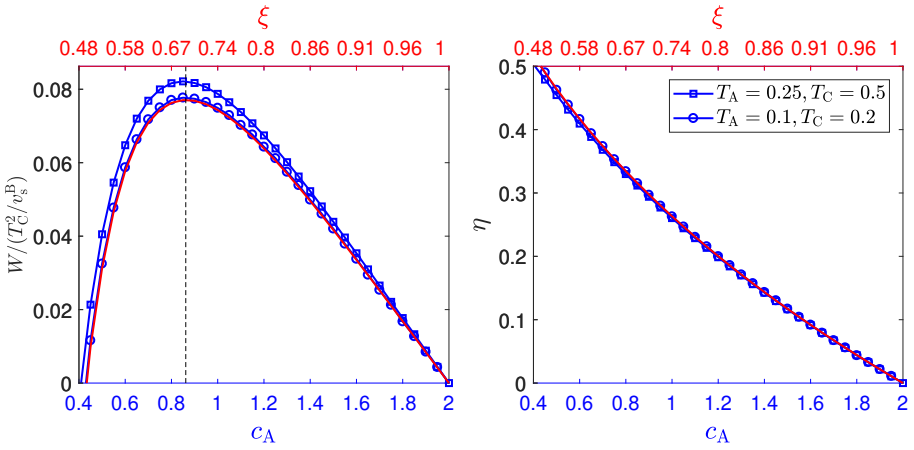

FIG. 1: **Work W and efficiency η vs interaction strength c_A.** The blue lines with squares and circles are obtained by numerically solving the TBA equation. The red solid lines in the left and right panels are obtained by Eqs. (35) and (38), respectively, where ξ for a given c_A is obtained by numerically calculating the sound velocities v_s^A and v_s^B at zero temperature [7]. The black dashed line corresponds to $\xi_c \approx 0.69$ for $\kappa = 0.5$ given by Eq. (37). In our numerical calculation, we set $n = 1$, $c_B = 2$, and $L = 1$.

The efficiency of the heat engine is

$$\begin{aligned} \eta &= 1 - \frac{Q_4}{Q_2} \\ &= 1 - \frac{v_s^B}{v_s^A}\frac{T_D^2 - T_A^2}{T_C^2 - T_B^2} \\ &= 1 - \xi\,. \end{aligned} \tag{38}$$

Especially, for the strong interaction case, the sound velocity is $v_s \approx 2\pi n\left[1 - 4(n/c) + 12(n/c)^2\right]$ [7], and thus the efficiency is given by

$$\eta \approx 1 - \frac{1 - \frac{4n}{c_A} + \frac{12n^2}{c_A^2}}{1 - \frac{4n}{c_B} + \frac{12n^2}{c_B^2}}\,, \tag{39}$$

which agrees with Eq. (20) in the thermodynamic limit. For the weak interaction case, the sound velocity is $v_s \approx 2n\left[(c/n) - (2\pi)^{-1}(c/n)^{3/2}\right]^{1/2}$ [7], and the efficiency is given by

$$\eta \approx 1 - \sqrt{\frac{c_A}{c_B}}\,. \tag{40}$$

The work output and the efficiency given by Eqs. (35) and (38) are universal at low energies for 1D system. Here we shall take 1D Bose gases as a platform to test these universal properties. For the interaction-driven engine with fixed particle number N and the length L studied in the present work, the sound velocity is changed during the two isoentropic strokes [(A to B) and (C to D)] by changing the interaction strength. We numerically calculate the work W and efficiency η for $\kappa = 0.5$ and $n = N/L = 1$. The interaction strength c_B is fixed at $c_B = 2$, which corresponds to the sound velocity $v_s^B \approx 2.50$. From Eq. (37), the optimal work is obtained at

$$\xi_c \approx 0.69 \tag{41}$$

for $\kappa = 0.5$. The numerical results are shown by the blue lines in Fig. 1. In the low temperature region, the numerical results are well explained by the results of the Luttinger liquid theory given by Eqs. (35) and (38), which are shown by the red solid lines. In the high temperature region, these two results deviate, which indicates the breakdown of the Luttinger liquid theory.

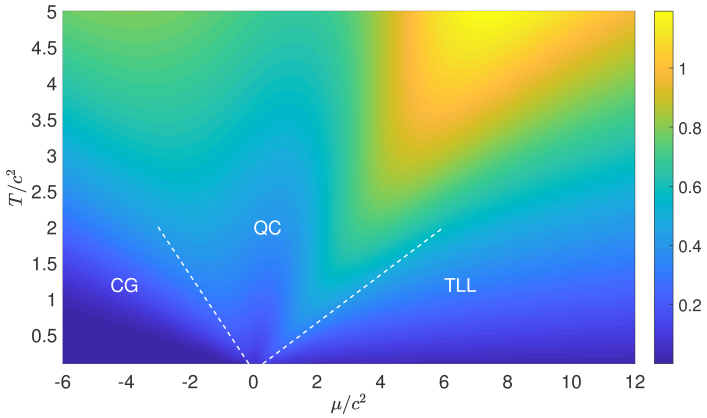

FIG. 2: **Phase diagram of the 1D Bose gas.** The color coding shows the specific heat. As the chemical potential μ is increased, the system undergoes a crossover from the classical gas (CG) to the Tomonaga-Luttinger liquid (TLL) across the quantum critical (QC) region.

Quantum criticality

The 1D Bose gases show rich critical properties in the plane of the temperature T and the chemical potential μ; see Fig. 2. In the so-called the Tomonaga-Luttinger liquid (TLL) region, where $\mu > 0$ and the temperature is below the right critical temperature, the magnitude of quantum and thermal fluctuations are comparable. In this region, the low-energy properties can be well captured by the Luttinger liquid theory and the excitation spectrum is given by $E = v_s|k|$, where v_s and k are the sound velocity and the wave vector, respectively. In the region of $\mu/T \ll 0$, i.e., the mean distance between atoms is much larger than thermal wave length, the system behaves as a classical gas (CG). A quantum critical (QC) region emerges between two critical temperatures (see the white dashed lines in Fig. 2) fanning out from the critical point $\mu_c = 0$. In this region, quantum fluctuation and thermal fluctuation have the same power of the temperature dependence. The density n is monotonically increasing with the chemical potential μ for a given temperature T and the interaction strength c. Therefore, one can go across the QC region from the CG to TLL regions only by increasing the density n of the working substance. Our numerical calculation shows W/N takes a maximum value in the crossover region between QC and TLL (see Fig. 3 in the main text).

Adiabatic processes versus quasi-static adiabatic processes

We consider a heat engine running through the interaction-driven quantum cycle shown in Fig. 1 in the main text. There are two heat sources with temperature T_A and T_C, where we assume $T_C > T_A$. The interaction strength is varied between c_A and c_B during the strokes B$\rightarrow$ C and C$\rightarrow$ D, with $c_B > c_A$. The average work per particle W/N is analyzed for differnet values of the density n of the working substance. In order to see the difference of the work output in the adiabatic and quasi-static adiabatic processes, we first numerically calculate the average work per particle done in a setting with $c_A = 1, c_B = 3, T_A = 1$ and $T_C = 5$. Figure (3) shows that there is an optimal work corresponding to a density n_c, denoted by dashed blacked lines. The critical value n_c increases as N increasing. In general, this optimal work exists in the thermodynamic limit, namely, $N \rightarrow \infty, L \rightarrow \infty$ and $n = N/L$ is finite. In this case, the n_c does not depend on N.

For the 1D interacting Bose gas, the scale-invariance does not hold for whole temperature regime. In Fig.(4), our numberical calculations show that the work output in the adiabatic processes (non-equilibrium states: A $\rightarrow$ B$'$,C$\rightarrow$ D$'$) is not the same as that in the quasi-static adiabatic processes (equilibirum states: A $\rightarrow$ B, C$\rightarrow$ D). Indeed, this difference does exist [8], but does not qualitatively change the work output of the heat engine, see Fig. 3. For a heat engine with fixed state parameters c_A, c_B, T_A and T_C, we observe that the optimizing work exists due to the change of the effective quantum statistics in the quantum critical region. The figure (4) suggests the quasi-static adiabatic processes can be used to qualitatively understand the optimizing work. Therefore, in the thermodynamics limit, we may use the quasi-static adiabatic processes instead of adiabatic processes to study the work output and efficiency of heat engine, also see Fig. 3 in the main text.

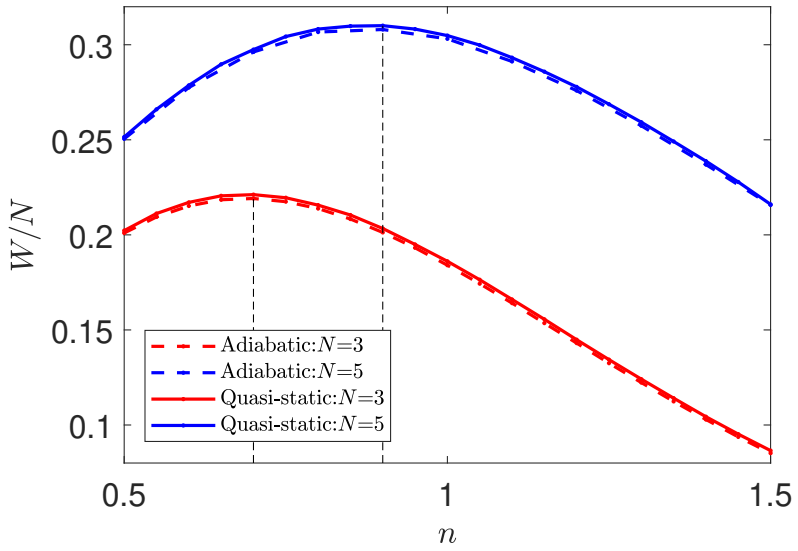

FIG. 3: Average work per particle W/N as a function of the density $n = N/L$ in an adiabatic process (dashed lines) and a quasi-static adiabatic process (solid lines) with different particle numbers. It shows existence of an optimal work for a characteristic value n_c of the density.

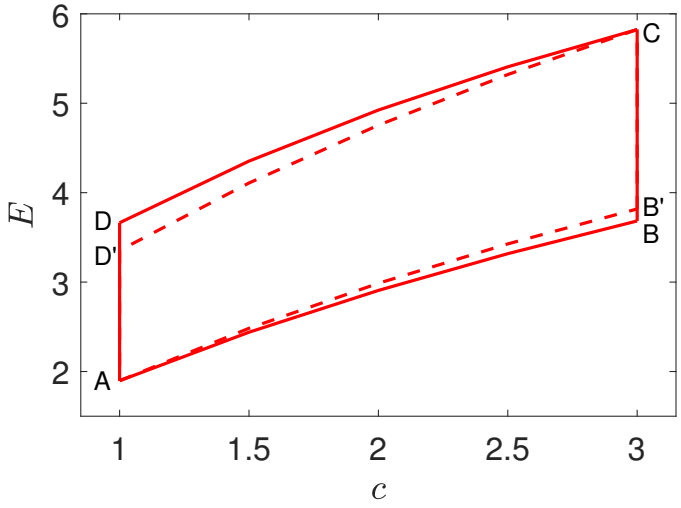

FIG. 4: Adiabatic driving versus quasi-static adiabatic driving in the interaction driven cycles. The stroke A$\rightarrow$ B (C $\rightarrow$ D) corresponds to the quasi-static adiabatic process, whereas A$\rightarrow$ B$'$ (C $\rightarrow$ D$'$) follows the non-equilibrium state associated with an adiabatic process. Here we set $T_{\rm A} = 1$, $T_{\rm C} = 5$, $N = 15$ and $L = 3.5$ for the numerical calculation.

V. 1D SPINOR FERMI GAS AS WORKING SUBSTANCE

Denoting by $\hat{P}^{\rm s}_{ij} = \frac{1}{4} - \hat{\mathbf{S}}_i \cdot \hat{\mathbf{S}}_j$ and $\hat{P}^{\rm t}_{ij} = \frac{3}{4} + \hat{\mathbf{S}}_i \cdot \hat{\mathbf{S}}_j$ are the projectors onto the subspaces of singlet and triplet functions of the spin arguments (σ_i, σ_j) for fixed values of all other arguments, the Hamiltonian of the system is given by [9, 10]

$$\hat{H}_{\rm SFG} = -\sum_{i=1}^{N} \partial^2_{x_i} + \sum_{1\le i<j\le N} [g_{\rm e}\delta(x_{ij})\hat{P}^{\rm s}_{ij} + v_{\rm o}(x_{ij})\hat{P}^{\rm t}_{ij}] \ . \tag{42}$$

Here, $v_{\rm o}$ is a strong, attractive, zero-range, and odd-wave interaction that is the 1D analog of 3D p-wave interaction. Similarly, $g_{\rm e}$ denotes the even-wave 1D coupling constant arising from 3D s-wave scattering [11]. The Hamiltonian of the spinor Fermi gas can be mapped to the Lieb-Liniger Hamiltonian [9] by promoting the coupling strength to an

operator dependent on the spin degrees of freedom

$$\hat{c} = 2^{-1}\left[(3c_{\rm o} + c_{\rm e})/2 + 2(c_{\rm o} - c_{\rm e})\hat{\mathbf{S}}_i \cdot \hat{\mathbf{S}}_j\right], \tag{43}$$

where the coupling constants $\{c_{\rm o}, c_{\rm e}\}$ are set by $g_{\rm e}$ and $v_{\rm o}$. The operator-valued coupling strength $\hat{c}$ can however be reduced to a real number $c = (3c_{\rm o} + c_{\rm e})/4 + (c_{\rm o} - c_{\rm e})\langle\hat{\mathbf{S}}_i \cdot \hat{\mathbf{S}}_j\rangle$ making use of a variational method that combines the exact solution of the LL model with that of the 1D Heisenberg models [9, 10]. As it turns out, this approximation is corroborated by the exact solution of (42) in a broad range of parameters [12]. Thus, the dependence of the interaction strength on the spin degrees of freedom provides a possible work outcoupling mechanism.

[1] M. Gaudin, Phys. Rev. A **4**, 386 (1971).
[2] M. T. Batchelor, X. W. Guan, N. Oelkers, and C. Lee, Journal of Physics A: Mathematical and General **38**, 7787 (2005).
[3] M. T. Batchelor and X.-W. Guan, Laser Physics Letters **4**, 77 (2007).
[4] J. Gemmer, M. Michel, and G. Mahler, *Quantum thermodynamics: Emergence of thermodynamic behavior within composite quantum systems*, vol. 784 (Springer, 2009).
[5] C. N. Yang and C. P. Yang, J. Math. Phys. **10**, 1115 (1969).
[6] X.-W. Guan and M. T. Batchelor, Journal of Physics A: Mathematical and Theoretical **44**, 102001 (2011).
[7] J. Yu-Zhu, C. Yang-Yang, and G. Xi-Wen, Chinese Physics B **24**, 050311 (2015).
[8] G. Xiao and J. Gong, Phys. Rev. E **92**, 012118 (2015).
[9] M. D. Girardeau, Phys. Rev. Lett. **97**, 210401 (2006).
[10] A. del Campo, J. G. Muga, and M. D. Girardeau, Phys. Rev. A **76**, 013615 (2007).
[11] M. Olshanii, Phys. Rev. Lett. **81**, 938 (1998).
[12] L. Guan, S. Chen, Y. Wang, and Z.-Q. Ma, Phys. Rev. Lett. **102**, 160402 (2009).